

Electric-field dependent conduction mechanisms in crystalline chromia

C.-P. Kwan, R. Chen, U. Singiseti, and J. P. Bird

Department of Electrical Engineering, University at Buffalo, Buffalo, New York 14260-1900, USA

(Received 10 February 2015; accepted 8 March 2015; published online 16 March 2015)

We investigate mechanisms of electric-field-induced conduction in high-quality chromia crystals. A crossover is observed between space-charge limited conduction and the Frenkel-Poole mechanism with increasing temperature, with the crossover occurring in the vicinity of the Neel temperature of this material. From an analysis of the Frenkel-Poole conduction, we infer the presence of charge traps that lie approximately 0.5 eV below the conduction-band edge. Our experiments confirm the excellent dielectric properties of chromia, a result that is important for attempts to utilize this material as a “gate” dielectric in future spintronic devices. © 2015 AIP Publishing LLC.
[<http://dx.doi.org/10.1063/1.4915309>]

Magnetolectrics (MEs) are attracting increasing interest due to their potential for application in post-CMOS spintronic devices.^{1,2} The characteristic feature of these materials is their capacity to exhibit a static magnetization in response to an applied electric field, or, equivalently, a static electrical polarization under the application of a magnetic field. As such, these materials offer a low-power route to the electrical control of magnetism, since the voltage-based switching of their magnetic states can be achieved with little accompanying flow of electrical current. This is since these materials are typically dielectrics, with high intrinsic resistivity that strongly limits current flow, even under the application of strong electric fields. MEs may therefore offer a route to replace the far-more energetically costly switching of magnetism by spin-transfer torque,³ and various proposals are currently being explored as a means to realize such technology. Particularly noteworthy are proposals to develop a ME-controlled magnetic tunnel junction, in which the rotation of free magnetic layer is accomplished via the exchange bias generated by a proximal ME.⁴⁻⁷

A ME with particular promise for application in spintronics is the antiferromagnetic insulator chromia (Cr_2O_3), which is one of a small number of materials capable of exhibiting ME response near room temperature.⁸⁻¹³ Recently, this material has been shown to exhibit a robust boundary magnetism at its (0001) interface, which may be exploited to provide a tunable exchange biasing of a thin ferromagnetic film.^{2,14} This advance represents a key first step towards the realization of the ME spintronic devices mentioned above.^{2,4-7}

Given the importance of chromia as an emergent material for electronics, surprisingly little is known about its different physical properties. Most importantly, there appear to be very few reports in the literature addressing the factors that govern the electrical characteristics of this material.¹⁵⁻¹⁸ For applications where voltage-based control of magnetism is envisaged this is potentially problematic, since electric-field control of the boundary magnetism of chromia relies implicitly on the absence of large leakage currents through the material. Motivated by this, in this letter we describe the results of experiments that we have performed to determine the resistivity of chromia, and to establish the dependence of its leakage current on electric field (applied voltage) and

temperature. Measurements performed on high-quality crystalline samples reveal the excellent insulating characteristics of this material, whose resistivity is found to be as large as 10–100 T Ω cm at room temperature. Our measurements reveal the presence of two mechanisms for field-dependent conduction, the relative strengths of which vary with temperature. From 200 to 300 K, measured current-voltage (I - V) characteristics are found to be consistent with the Mott-Gurney model¹⁹ for space-charge limited conduction (SCLC). With increasing temperature, the mobility due to this mechanism grows exponentially, and current flow via the Frenkel-Poole (FP)²⁰ mechanism dominates from 300 to 400 K. Associated with field induced activation out of charge-trapping sites, an analysis of the current in the FP regime allows us to infer the characteristic energy of these traps. Inferred energies (~ 0.5 eV) are found to be consistent with the results of a recent independent study, where the traps were attributed to oxygen vacancies in the chromia crystal.²¹ Overall, our measurements suggest that chromia possesses excellently suited characteristics for the realization of voltage control of magnetism. They also provide important benchmarking figures that may be used to assess the quality of the epitaxially grown chromia thin films²²⁻²⁴ that will ultimately be needed for spintronic-device fabrication.

High-quality (0001) chromia crystals were purchased from crystal GMBH. The two crystals were each 0.5 mm thick, with length and width of 4- and 2-mm, respectively. In order to allow electrical measurements of the high-resistivity material, the crystals were thinned down in a mechanical polisher. Sample A was reduced to a thickness of just 70 μm , while sample B was thinned down to 110 μm . Following this step, 100 nm of gold was evaporated onto the top surface of the crystals, which were then glued with silver paste into a plastic dual-in-line (DIP) package. The top surface of the crystals was then contacted by means of a gold wirebond, following which the DIP packages were mounted on the cold finger of a JanisTM closed-cycle cryostat. Current-voltage characteristics were then measured using an HP 4155B Semiconductor Parameter Analyzer, with an input impedance of $\geq 10^{13}$ Ω . Due to the high intrinsic resistance (T Ω) of the samples, care was needed to eliminate parasitic paths to ground in the measurement circuit, which might otherwise

yield spurious resistance estimates. Most importantly, the entire measurement setup was calibrated by determining the resistance of an open circuit on the same DIP package, and measuring this leakage resistance over the full temperature range of the experiments (200–400 K). The influence of this background leakage was found to be largest at the low-temperature end of our measurement range, where it contributed no more than 5% of the current measured with the samples present. At higher temperatures, this contribution was even smaller. In the discussion that follows, we present the results of detailed temperature-dependent studies of sample A. While sample B was measured over a narrower temperature range (290–350 K), it was nonetheless found to exhibit behavior consistent with that of sample A. Our measurements were made by first cooling to 200 K under zero-field conditions (i.e., no applied electric or magnetic field), following which current-voltage characteristics were recorded as temperature was increased in a series of steps to 400 K. Resistivity values, determined at room temperature and for various voltages, were in the range of 10–100 T Ω cm for the two samples.

In the main panel of Fig. 1, we plot the I - V characteristic of sample A, measured over a number of temperatures from 200 to 400 K. The corresponding behavior exhibited by sample B is plotted in the inset, for the narrower range of temperature from 290 to 350 K. It is clear that from the behavior shown in the two plots that the current is a strongly nonlinear function of voltage, and that is also strongly dependent on temperature (T). Such behavior is typical of dielectrics, in which bulk conduction is typically dominated by SCLC and the FP mechanism.²⁵ In the case of SCLC, the current density (J) is expected to vary with voltage as

$$J = \frac{9\epsilon_r\epsilon_0\mu}{8d^3} V^2, \quad (1)$$

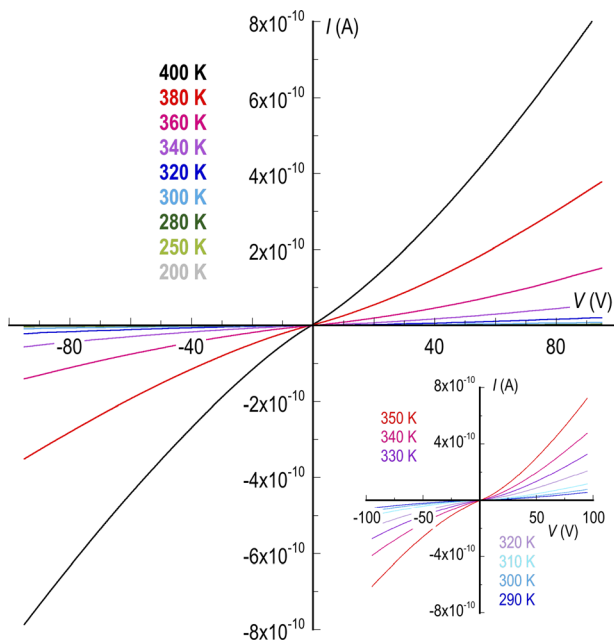


FIG. 1. The main panel plots the I - V curves of sample A at various temperatures from 200 to 400 K. The inset plots I - V curves of sample B at seven different temperatures from 290 to 350 K.

where ϵ_r is the dielectric constant, ϵ_o is the permittivity of free space, μ is the carrier mobility, and d is the insulator thickness. Separately, the FP mechanism yields a contribution

$$J \propto \frac{V}{d} \exp \left[-q \left(\frac{\phi_t - \sqrt{qV/d\pi\epsilon_r\epsilon_o}}{k_B T} \right) \right], \quad (2)$$

where $q\phi_t$ is the depth (measured from the conduction-band edge) of the traps responsible for the field-assisted emission.

Dependent upon the temperature range of our measurements, we find clear evidence for both SCLC and the FP mechanism. We begin by discussing the role of the latter contribution, which appears to dominate the current at temperatures above the Neel temperature of 308 K. To illustrate this point, we note from the form of Eq. (2) that, under conditions where ϕ_t is only weakly dependent on voltage, the FP mechanism should be revealed as a straight line in a plot of $\ln(J/V)$ vs. $V^{0.5}$. This behavior is clearly demonstrated in Fig. 2(a), where we plot I/V vs. $V^{0.5}$ from 340 to 400 K and clearly observe the expected straight line dependence. It is apparent from this (semi-log) plot that the onset of the FP behavior occurs at lower voltages at increased temperatures; this is consistent with the fact that the field-assisted emission from the localized traps should be easier to induce at higher temperatures, in accordance with Eq. (2).

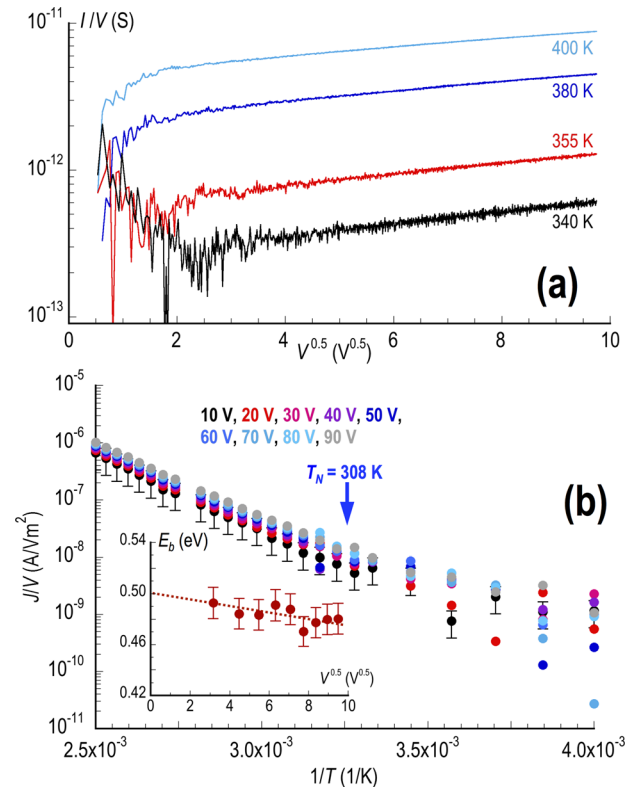


FIG. 2. (a) I - V curves of sample A, replotted in a manner to reveal the connection to the FP mechanism described by Eq. (2). (b) The main panel plots J/V vs. $1/T$ at various fixed voltages (indicated), in order to reveal the temperature-dependent behavior predicted by the FP mechanism. The Neel temperature (T_N) of 308 K is also indicated on the plot. For the sake of clarity, error bars are indicated for the 10 V data only. The inset plots the variation of E_b vs. $V^{0.5}$, which extrapolates to an intercept that corresponds to the trap depth $q\phi_t = 0.5$ eV.

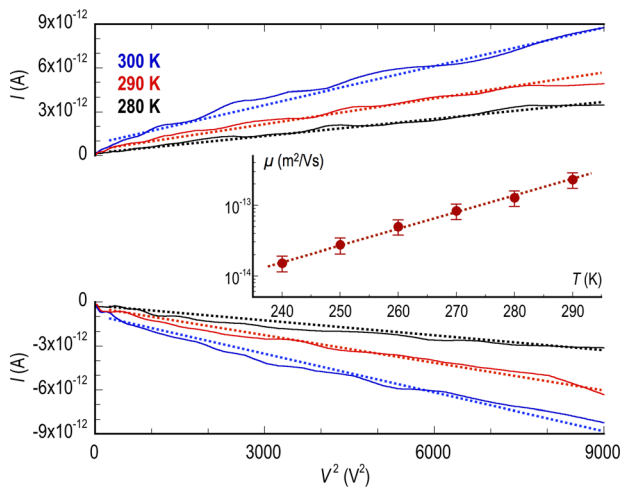


FIG. 3. The main panel (upper and lower parts) plots I vs. V^2 for sample A at three different temperatures to indicate the connection to SCLC. The dotted lines through each data set indicate a straight-line variation predicted by Eq. (1). The inset plots the mobility inferred from the slope of the straight lines, as a function of temperature. The data fall on a straight (dotted) line, indicating an exponential increase with temperature.

For a more accurate analysis of the FP mechanism, we note that Eq. (2) predicts that a plot of $\ln(J/V)$ as a function of $1/T$ (at fixed V) should yield a straight line with a slope that is equal to an “effective trap depth”¹⁸

$$E_b = -q(\phi_t - \sqrt{qV/d\pi\epsilon_r\epsilon_0}). \quad (3)$$

In Fig. 2(b), we show plots of J/V (on a logarithmic scale) vs. $1/T$ for various voltages from 10 to 100 V. Clearly, the data fall on a good straight line over a reasonably wide temperature range that extends from around 300 to 400 K. At lower temperatures than this the data fall away from the straight line, suggesting that another mechanism instead becomes dominant. To emphasize the connection to Eq. (3), in the inset to Fig. 2(b) we plot the variation of E_b as a function of $V^{0.5}$. The data points shown in this plot were computed from the straight-line slope of the various data sets in the main panel, by assuming a dielectric constant $\epsilon_r = 11$.¹³ By extrapolating the data to $V=0$ we infer $q\phi_t = 0.5$ eV, a value in good agreement with that reported in independent measurements of low energy electron diffraction (LEED) in chromia.²¹ In that work, the source of the traps was attributed to oxygen vacancies in the crystal structure. We also note that the slope of the line in the inset implies a dielectric constant $\epsilon_r = 13 \pm 3$, a value consistent with our original assumption of $\epsilon_r = 11$.

TABLE I. Reported resistivity values for chromia thin films.

References	T (K)	ρ^a (Ω cm)	Comments
15	300	10^2 – 10^4	Sputter deposited thin films of thickness 2–600 nm
16	300	$\leq 10^9$	130-nm thick films formed by pulsed-laser deposition
17	300	10^7	140–300-nm thick films formed by thermal evaporation of Cr powder
18	313–373	...	Current-voltage characteristics reported for sputtered Cr_2O_3 (15-nm) resistive-random-access-memory structures
30	500	10^2 – 10^3	500–600-nm thick polycrystalline films prepared by normal pressure chemical vapour deposition
31	300	10^2 – 10^4	AC conductivity was measured for nanostructured chromia films synthesized by the hydrothermal technique
This work ^b	200–400	5×10^{15} – 4×10^{12}	Measurements of thick chromia crystals

^a ρ is the film resistivity.

^bResistivity values quoted are for a source voltage of 1 V.

Turning next to the behavior at lower temperatures, in the range of 200–290 K, this is found to be more consistent with that expected for SCLC. We indicate this in Fig. 3, in the main panels of which we plot current as a function of V^2 to reveal the straight-line behavior predicted by Eq. (1). From the slope of the resulting straight line, we are able to extract the carrier mobility and its dependence on temperature, and the results of this analysis are plotted in the inset to Fig. 3. The data nicely follow an exponential dependence, behavior that is typical of many insulators (see, for example, Refs. 26–29).

At the same time that we have clarified the mechanisms for field-induced conduction in chromia, our measurements also reveal the excellent insulating characteristics of this material. As noted already, room-temperature resistivity values are in the range of 10–100 T Ω cm, dependent upon the applied voltage (electric field). These values are significantly higher than those reported in studies of various chromia films. Wu and Winterbottom,¹⁵ for example, formed submicron thickness chromia films by sputter deposition of chromium-oxide coatings and reported room-temperature resistivity of 10^2 – 10^4 Ω cm. Lim *et al.*¹⁶ similarly used pulsed-laser film deposition and reported resistivity values as large as 10^9 Ω cm. In a more recent study, Julkarnain *et al.*¹⁷ formed chromia films by thermal evaporation of Cr powder, and found them to exhibit room-temperature resistivity of 10^7 Ω cm. Clearly, all of these values are significantly lower than those reported here, which suggests that much still needs to be done to synthesize high-quality chromia films that can approach the insulating quality of bulk crystals. This point is further made clear in Table I, where we summarize the results of earlier studies of chromia’s electrical resistivity.^{15–17,30,31} Clearly, these prior values are much smaller than those demonstrated here. It has been pointed out previously that the Neel temperature of chromia films may serve as a reliable indicator of their quality.³² The measurements here suggest that the resistivity may be added as a useful parameter that may also serve this purpose. An important question that we have been unable to address here, where we have explored conduction along the chromia c -axis, concerns any possible dependence of chromia’s electrical properties on crystal orientation.

An intriguing aspect of our study is the crossover from SCLC to the FP mechanism, which occurs near the Neel temperature (T_N) for chromia. The current-voltage characteristics indicate that the conduction is significantly enhanced

beyond this temperature. The mechanism responsible for this increased conductivity is currently unclear and is puzzling given that the SCLC and FP mechanisms are not expected to depend explicitly upon magnetic degrees of freedom. One interpretation might be that the magnetic ordering that occurs below T_N is accompanied by subtle structural changes that alter the energy of the defect states involved in the PF transport. While we currently have no evidence to suggest that this is indeed the case, we do note that Raman studies of other antiferromagnets have shown the phonon frequencies of such materials to be modified by the onset of antiferromagnetic order.³³

In conclusion, we have investigated the mechanisms of electric-field-induced conduction in high-quality chromia crystals. A crossover is observed between SCLC and the FP mechanism with increasing temperature, with the crossover occurring in the vicinity of the Neel temperature (308 K (Refs. 8–13)) of this material. From an analysis of the FP conduction, we infer the presence of charge traps that lie approximately 0.5 eV below the conduction-band edge. The SCLC is described by a strong (exponentially) temperature-dependent mobility, consistent with observations for other insulators. Overall, our experiments confirm the excellent dielectric properties of chromia, a result that is important for attempts to utilize this material as a “gate” dielectric.¹⁴ The results presented here furthermore provide important benchmarking data that can be used to assess the quality of epitaxial chromia in potential device applications.

This project was supported by the Semiconductor Research Corporation through the Center for Nanoferroic Devices (CNFD), an SRC-NRI Nanoelectronics Research Initiative Center under Task ID 2398.001.

¹D. E. Nikonov and I. Young, *Proc. IEEE* **101**, 2498 (2013).

²P. A. Dowben, C. Binek, and D. E. Nikonov, “The potential of nonvolatile magnetoelectric devices for spintronic applications,” in *Silicon Nanoelectronics*, 2nd ed., edited by S. Oda and D. K. Ferry (Taylor and Francis, CRC Press, 2015).

³F. Jonietz, S. Mühlbauer, C. Pfleiderer, A. Neubauer, W. Münzer, A. Bauer, T. Adams, R. Georgii, P. Böni, R. A. Duine, K. Everschor, M. Garst, and A. Rosch, *Science* **330**, 1648 (2010).

⁴Ch. Binek and B. Doudin, *J. Phys.: Condens. Matter* **17**, L39 (2005).

⁵X. Chen, A. Hochstrat, P. Borisov, and W. Kleemann, *Appl. Phys. Lett.* **89**, 202508 (2006).

⁶M. Bibes and A. Barthelemy, *Nat. Mater.* **7**, 425 (2008).

⁷W. Kleemann, *J. Appl. Phys.* **114**, 027013 (2013).

⁸T. J. Martin and A. C. Andersen, *IEEE Trans. Magn.* **2**, 446 (1966).

⁹H. B. Lal, R. Srivastava, and K. G. Srivastava, *Phys. Rev.* **154**, 505 (1967).

¹⁰E. Kita, A. Tasaki, and K. Siratori, *Jpn. J. Appl. Phys., Part 1* **18**, 1361 (1979).

¹¹Y. F. Popov, A. M. Kadomtseva, D. V. Belov, G. P. Vorob'ev, and A. K. Zvezdin, *JETP Lett.* **69**, 330 (1999).

¹²P. Borisov, A. Hochstrat, V. V. Shvartsman, and W. Kleemann, *Rev. Sci. Instrum.* **78**, 106105 (2007).

¹³A. Iyama and T. Kimura, *Phys. Rev. B* **87**, 180408(R) (2013).

¹⁴X. He, Y. Wang, N. Wu, A. N. Caruso, E. Vescovo, K. D. Belashchenko, P. A. Dowben, and C. Binek, *Nat. Mater.* **9**, 579 (2010).

¹⁵R. C. Ku and W. L. Winterbottom, *Thin Solid Films* **127**, 241 (1985).

¹⁶S.-H. Lim, M. Murakami, S. E. Lofland, A. J. Zambano, L. G. Salamanca-Riba, and I. Takeuchi, *J. Magn. Magn. Mater.* **321**, 1955 (2009).

¹⁷M. D. Julkarnain, J. Hossain, K. S. Sharif, and K. A. Khan, *J. Optoelectron. Adv. Mater.* **13**, 485 (2011).

¹⁸S.-C. Chen, T.-C. Chang, S.-Y. Chen, H.-W. Li, Y.-T. Tsai, C.-W. Chen, S. M. Sze, F.-S. Yeh (Huang), and Y.-H. Tai, *Electrochem. Solid-State Lett.* **14**, H103 (2011).

¹⁹N. F. Mott and R. W. Gurney, *Electronic Processes in Ionic Crystals* (Clarendon Press, Oxford, 1940).

²⁰J. Frenkel, *Phys. Rev.* **54**, 647 (1938).

²¹S. Cao, N. Wu, W. Echtenkamp, V. Lauter, H. Ambaye, T. Komesu, C. Binek, and P. A. Dowben, “The surface stability of Cr₂O₃(0001),” *J. Phys. Cond. Matt.* (submitted).

²²M. Audronis, A. Matthews, and A. Leyland, *J. Phys. D: Appl. Phys.* **41**, 035309 (2008).

²³K. Pedersen, J. Böttiger, M. Sridharan, M. Sillassen, and P. Eklund, *Thin Solid Films* **518**, 4294 (2010).

²⁴P. M. Sousa, A. J. Silvestre, and O. Conde, *Thin Solid Films* **519**, 3653 (2011).

²⁵S. M. Sze and K. K. Ng, *Physics of Semiconductor Devices*, 3rd ed. (John Wiley & Sons, Inc., 2007).

²⁶P. W. M. Blom, M. J. M. de Jong, and M. G. van Munster, *Phys. Rev. B* **55**, R656 (1997).

²⁷H. Siringhaus, P. J. Brown, R. H. Friend, M. H. Nielsen, K. Bechgaard, B. M. W. Langeveld-Voss, A. J. H. Spiering, R. A. J. Janssen, E. W. Meijer, P. Herwig, and D. M. de Leeuw, *Nature* **401**, 685 (1999).

²⁸L. Bozano, S. A. Carter, J. C. Scott, G. G. Malliaras, and P. J. Brock, *Appl. Phys. Lett.* **74**, 1132 (1999).

²⁹W. Brütting, S. Berleb, and A. G. Mückl, *Synth. Met.* **122**, 99 (2001).

³⁰C.-S. Cheng, H. Gomi, and H. Sakata, *Phys. Status Solidi A* **155**, 417 (1996).

³¹M. M. Abdullah, F. M. Rajab, and S. M. Al-Abbas, *AIP Adv.* **4**, 027121 (2014).

³²X. He, W. Echtenkamp, and Ch. Binek, *Ferroelectrics* **426**, 81 (2012).

³³C. Binek and W. Kleemann, *J. Phys.: Condens. Matter* **4**, 65 (1992).